

Features of Processing Signals from Stationary Radiation Sources in Multi-Position Radio Monitoring Systems

Volodymyr Druzhynin¹[0000-0002-5340-6237], Serhii Toliupa²[0000-0002-1919-9174],
Oleksandr Pliushch³[0000-0001-5310-0660], Mikhailo Stepanov²[0000-0001-6376-4268],
and Bohdan Zhurakovskiy¹[0000-0003-3990-5205]

¹National Technical University of Ukraine “Igor Sikorsky Kyiv Polytechnic Institute,” Ukraine

²Taras Shevchenko National University of Kyiv, Ukraine

³State University of Telecommunications, Ukraine

vladimirdruzhinin68@gmail.com

Abstract. This paper performs an analysis of the movement impact of radio monitoring system receiving elements on this system’s functional capabilities. The analysis is done in the context of space-time processing of the signals that arrive from *a priori* unknown stationary radio-emitting sources. It is accentuated that at present both identification of the legitimate transmitters and establishing the presence and the locations of illegitimate ones, which are paramount tasks of radio monitoring, become more and more complicated due to the introduction of new technologies with irregular spectrum use. A new method is proposed to determine the coordinates of those illegitimate sources in the passive monitoring mode with non-directional reception. For the method, a technique is designed of finding positions of signal reception points during the radio monitoring interval to unambiguously determine radio emissions bearings in the passive mode and radio receivers’ movement in an *a priori* calculated space configuration. The proposed method and algorithms have an economic advantage over space systems with similar tasks and can substantially improve efficiency in certain conditions.

Keywords: Radio Monitoring, Passive Monitoring Mode, Monitoring Interval, Non-Directional Reception, Emissions’ Bearings.

1 Introduction

1.1 Analysis of Challenges in Identifying Legitimate Sources of Emissions during Radio Monitoring Process

At present, radio frequency monitoring (RFM) is a very difficult and resource-consuming task due to the density of the spectrum used by the communication systems with multiple access, such as mobile cellular ones. Trends and features of technical deployment, which the current and prospective mobile communication technologies possess, impose further restrictions on the RFM process. Among the main factors that hinder RFM of the spectrum use, some are more important than others.

Copyright © 2020 for this paper by its authors.

Use permitted under Creative Commons License Attribution 4.0 International (CC BY 4.0)

Firstly, it is a deployment of wideband and ultra-wideband communication channels with a concomitant reduction in the radiation power of their transmitters. This trend seems to be the most important feature of current and prospective technologies development. The trend is shaped by the fact that communication systems are no longer the systems that provide only communication services for the subscribers; rather, they show signs of being control and monitoring elements for the complex infrastructure objects, such as a city with its road, municipal, social and other networks for population life activities and industrial production. In this case, communication network infrastructure ought to reflect the features of the surrounding ones and is an organic part of the general control and monitoring system (so-called ecosystem). In such a system, broadband communication channels are, to a certain extent, like blood vessels (pipelines) that secure transmission and reception of large volumes of information that is transferred between the general infrastructure elements. Already currently, fourth-generation mobile networks, which use LTE-Advanced technology, have a bandwidth of 20 MHz, while fifth-generation communication systems are expected to deploy channel bandwidths up to 100 MHz and beyond, depending on the frequency band. Besides, the narrowband communication systems, such as those of the second generation ones (GSM technologies), will linger on; their channels will be used for data transfer in the general topology of promising communication networks.

Use of wideband communication channels is enabled due to the available radio frequency resources (RFR) in the super-high frequency (SHF) band, such as 26 GHz, and extremely high frequency (EHF) band, such as 40 and 70 GHz (according to CEPT research). Transition to these bands implies use, among the others, of the antennas with narrow beam directivity patterns (NBDP), which considerably complicates RFM implementation.

Secondly, big challenges for RFM are created by the introduction of adaptive modes of transmitters' operation in both frequency-time and space domains of the emitted signals. Modern and prospective mobile communication systems use the multiple access method based on orthogonal frequency division multiple access (OFDMA) technique in combination with the redistribution of frequency resources between the base station sectors, as well as the deployment of multi-antenna/multi-channel space emissions (MIMO) for the base station and the user equipment. Adaptation to the end-users demands as well as propagation media conditions is achieved at the expense of active antenna systems (AAS) based on phased antenna arrays (PAA); this approach makes it possible to amplify emitted signals in the required direction for a certain user. This changing nature of the emission parameters necessitates more meticulous and prolonged monitoring of the transmitters' characteristics using RFM.

Thirdly, implementation of the so-called "technological neutrality" (TN) allows the carriers to effectively use licensed frequency band as they see fit: in mobile or fixed modes of operation, with time-division (TTD) or frequency division duplexing (FDD) and different multiple access technologies for the users. Thus, emission parameters monitoring should expect changes in radiation parameters and a necessity of controlling the operator's compliance with the demands in the adjacent frequency bands while using those different technologies. Such requirements concern, as a rule, restrictions on the out-of-band emissions in the transmitters (control of a block edge mask (BEM),

which is a transmitter spectrum mask that applies at the edge of a contiguous licensed block of the spectrum), as well as filtration (if applicable) in adjacent receivers.

Fourthly, general changes in the electromagnetic environment in a certain location or a city subjected to RFM are linked to multi-standard frequency use by the operators due to deployment of promising machine type communications (MTC), which implement projects of Internet of things (IoT) and machine-to-machine communications (M2M); these connections are achieved through typical technological communication channels of the modern mobile systems in all available frequency bands and channels including in prospective fifth-generation technologies and frequencies allocated for them. A feature of an MTS operation is that the synchronization and the power in the transmission channel, which, in contrast to the conventional communication channel, are defined by a separate timetable by the tasks of an infrastructure element.

On the background of the drastic changes in the electromagnetic environment, there will continue to operate during the transition period a lot of technological communication stations with typical radiation parameters, as well as low-powered transmitters of wide-band internet access (WBIA), stations of radio-relay and conventional radio communications, repeaters in mobile systems and so on; they will require separate detailed radiation inspection with the aim of establishing the legality of transmitters operation and observance of the use of RFR.

The outlined major factors that shape the electromagnetic environment of the future create uncertainty as to transmitters' emission parameters, which in contrast to the conditions of the environment created by the previous technologies can be described as irregular spectrum use. This irregular spectrum use substantially changes the tasks of the RFM that are concerned with transmitters identification, and their legality of RFR use, and radiation parameters radio monitoring. In the conditions of constant radiation parameters variation and multi-standard spectrum use, a certain risk of en mass utilization of the frequencies by the illegitimate network transmitters emerges; radiation parameters of those transmitters will also be variable but masked by the general background emissions of the legitimate radiations of the changeable nature, which is the main feature of the network as a whole. A part of the whole radio resource of the transmitter, which serves a certain sector of the base station, can be used in another sector, thus making identification and assessment of transmitter parameters impossible because of the weak signal at the moment of the scheduled measurement. Similarly, emissions of an illegal transmitter (for example a repeater) can be hidden in the special schedule of the RFR exploitation, which envisions redistribution of the frequency resource and its multi-standard utilization. Only a detailed analysis of the whole licensed operator's spectrum both in the coverage area and in the immediate vicinity to the base station permits to collect of additional information for the transmitter identification.

Thus, as the analysis indicates, the task of transmitter identification in the conditions of introduction and development of the new technologies is topical, one of the most difficult to deal with, and needs an urgent solution.

1.2 Analysis of Challenges for a Search for Interference Sources in the Current Electromagnetic Environment

Search for sources of interference in the previously described conditions is no less difficult than the identification of the legitimate transmitters and their parameter measurement. Those sources are also masked by the irregular nature of the RFR utilization. But the interfering sources can be both illegitimate transmitters and legitimate ones that simply do not abide by the radiation parameters specified for a certain technology, as well as the limitations that are imposed as a result of compatibility study with the transmitters in the neighboring frequency band of another operator. Transmitter identification by the data from the network identifiers and those of certain base stations or their sectors will permit to carry out a more detailed analysis of signal spectra in the ambient environment of an interference location and finally reveal the interfering signal from an illegitimate transmitter (for example, a repeater). In general, to search for the source of interference, it is necessary to reduce general uncertainty as to the radiation parameters of the transmitters by the way of using additional information concerning that interference from the complaining affected legitimate user and some preliminary measurements at the site of the interference manifestation. In this case, by increasing the power of the interference relative to the useful signal, the RFM receiver has a chance to do a more targeted and detailed analysis of the interference spectrum and, thus, secure better precision and reliability of the results of the spectrum analysis and measurements.

For the described reasons, a search for an interference source in the conditions of irregular spectrum use demands long and meticulous work and presents itself as a difficult and topical challenge.

2 Impact of the Dynamic Factors on the Operation of Airborne Radio Monitoring Systems with One Element

2.1 The Case of Unchanging Speed and Course of the Airborne Element

It is well-known [1–4] that dynamic factors of airborne RFM systems operation have a substantial effect on their efficiency of practical applications. This is especially so for passive systems of RFM. Let us assume that a remotely controlled aerial vehicle (RCAV) with an onboard radio receiving module (RRM) is moving in a fixed direction with a constant speed \vec{V}_{RRM} .

At a certain time instant t_i , the signal emitted from an *a priori* unknown radio emission source (RES) comes from a previously unknown angle α_1 to the input of the RRM antenna (Fig. 1).

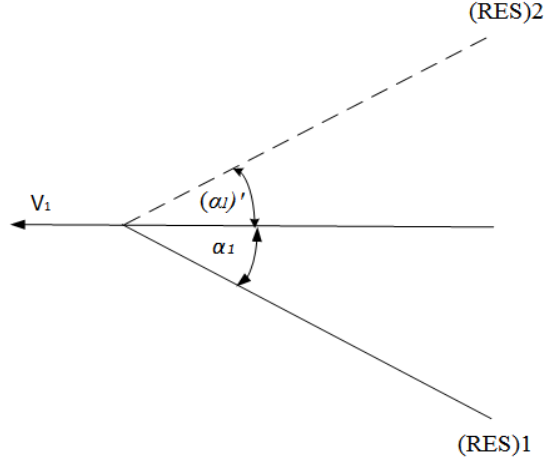


Fig. 1. Explanation of the ambiguous bearing of the signal from the RES in the conditions of non-directional reception.

In this case, the equation for the carrier frequency of the received signal is as follows:

$$f_{(n)rec} = f_n \left(1 + \frac{V_{RRM}}{c} \cos \alpha_1 \right) \quad (1)$$

where f_n is signal carrier frequency; c is light speed; V_{RRM} is the movement speed of RRM of RCAV [3].

If the frequency of the signal carrier f_n and the traveling speed of RCAV V_{RRM} are *a priori* known, then, after measuring $f_{(n)rec}$, it is possible to determine the bearing of the radio emission source (angle α):

$$\alpha_1 = \arccos \left[\frac{c}{L/T} \left(\frac{f_{(n)rec}}{f_n} - 1 \right) \right]. \quad (2)$$

It is necessary to stress that the accuracy of the bearing for a RES depends upon the length of L (the synthesized aperture) and the corresponding distance that is covered by RRM during the monitoring time T .

The advantage of such systems is that they secure high accuracy of signal-bearing measurement with the use of antennas with a small aperture. On the downside, determining the bearing is possible only if the radiation spectrum is known in advance. This factor greatly limits the use of the monitoring systems with a synthesized aperture.

2.2 Case of Changing Speed and Course of the Airborne Element

The situation described in the previous subsection can be resolved in the case in which the speed of the RRM movement is changed either by the absolute value or by the direction. This causes corresponding changes in the Doppler frequency during the monitoring time T .

If RRM moves in the fixed direction with the velocity $V(t)$ changing by module, then the harmonic wave from the interference with the frequency f_n is registered at the output of the receiving element as a frequency modulated oscillation and its time function is described by the following equation [3]:

$$f_{rec} = f_n \left(1 + \frac{V(t)}{c} \cos\alpha \right) \quad (3)$$

If the speed of the receiving element $V(t)$ observes harmonic function with the frequency f_n , then (3) can be presented as [3]:

$$f_{rec} = f_n \left(1 + \frac{V_0}{c} \cos(2\pi f_n t) \cos\alpha \right) \quad (4)$$

where V_0 is the amplitude of the movement speed of RRM.

The amplitude of the fluctuation of the Doppler frequency of the incoming registered oscillations (F_D) and the average frequency of these oscillations (f_{aver}) are described as follows [3]:

$$\begin{cases} F_D = f_n \frac{V_0}{c} \cos\alpha \\ f_{aver} = f_n \end{cases} \quad (5)$$

In this case, the frequency and arrival angle of the incoming signal can be found based on the measurements of frequency fluctuation amplitude and the average frequency of the registered oscillations. The accuracy of the bearing of the incoming oscillation depends on the amplitude of the receiving element movement.

It is necessary to stress that this phenomenon will take place as well in those cases when changes of the RRM velocity according to the laws differing from the harmonic one.

Let us consider the case in which RRM during the period t_1 moves in the fixed direction with the constant speed V_1 , and then during the period t_2 is in a changed fixed direction with the constant speed V_2 (Fig. 2).

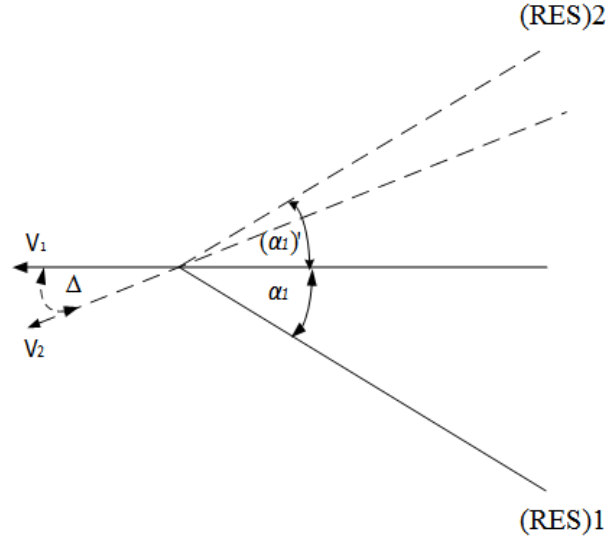


Fig. 2. The geometrical ratio of the angles for the situation with the changes in the movement direction for the airborne RRM.

The feature of the first two models (1) and (4) is the ambiguity in the bearings measurements: signal coming from the symmetrical directions (from the angles α_1 and α_2) in Fig. 1, are indistinguishable.

In the case in question (Fig. 3), the situation is different from those above.

When the RRM moves in the first direction, the registered Doppler frequency is described by the equation:

$$F_{D1} = f_n \frac{V_1}{c} \cos \alpha_1, \quad (6)$$

and when it moves in the second direction (Fig. 2) by this one:

$$F_{D2} = f_n \frac{V_2}{c} \cos(\alpha_1 + \Delta) \quad (7)$$

If V_1 , V_2 and Δ are *a priori* determined by the spatial configuration of the radio monitoring system, and F_{rec1} and F_{rec2} are the values that are measured, then the bearing of the signal from RES and its frequency can be unambiguously determined using the above equations (6) and (7).

In this case, the accuracy of parameters measurement from the signal of RES depends upon velocity values V_1 , V_2 and the angle Δ .

3 Design of the Novel Dynamic Model of Space-Time Processing of Signals from RES

Basing on the above-presented mathematic apparatus, this paper proposes a dynamic model of space-time processing of signals from RES in the conditions of their space diversity reception by the moving RRM with *a priori* has known space parameters on the monitoring time interval.

Currently, mobile means of monitoring are capable to functionally complement stationary ones and secure flexible support of effective radio monitoring while carrying out measurements of the radio emissions that are out of reach for the stationary ones by using potential capabilities of the synthesized aperture in passive systems [5–9].

Fig.3 illustrates space locations of two signal reception points (A and B) relative to RES. In this case, monitoring of the RES is performed by two moving RRM, which move with velocities V_1, V_2 and are located at a distance one from the other. The reception points (A and B) of the signal from the directions α_1, α_2 are located within the scope of the main lobe of the directivity pattern of the RES in both vertical and horizontal planes.

Fig. 3 enables the design of an algorithm to calculate coordinates of the RES ($x_{RES}; y_{RES}$) in the passive mode of monitoring for non-directional reception for the set of input data.

The input data for the algorithm are:

1. Location coordinates for RRM 1 and RRM 2 throughout RES monitoring.
2. Delay time (t_d) of the RES signal arrival to the point *B* relative to the time of RES signal arrival to the point *A*.
3. Distance (d) and interval (I) are non-changing during the monitoring time (T) of the RES.
4. $V_1 = V_2$.

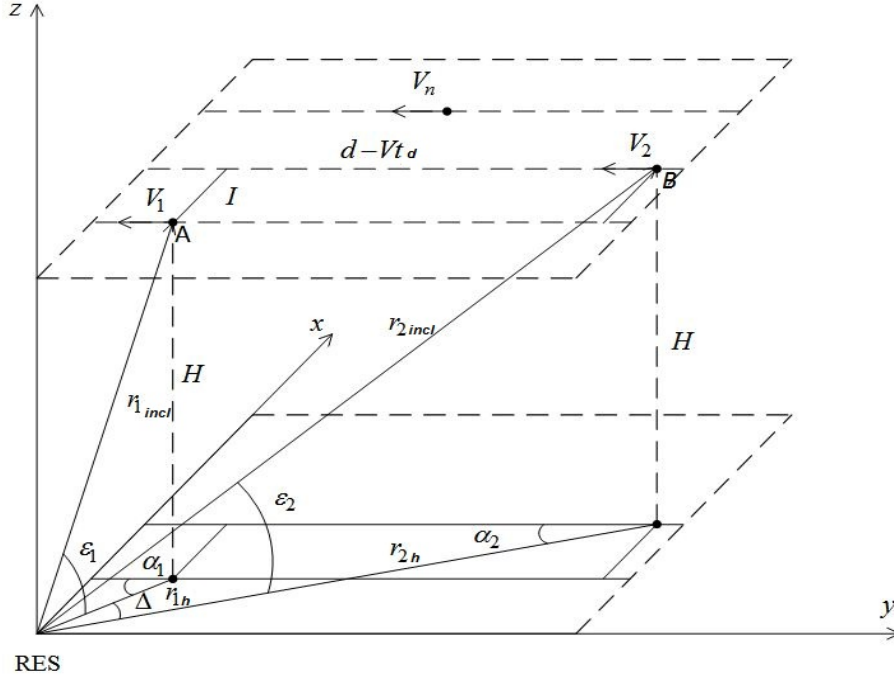


Fig. 3. The trajectory of the movement of the two RRM by parallel courses with a specified distance (d) and interval (I) between their carriers.

Algorithm of determining RES location coordinates ($x_{RES}; y_{RES}$) in the passive mode of monitoring can be broken down into the following steps.

Firstly, let us determine the power of the RES (P) and the angle between directions of the movement of the receiving elements ($\Delta = \hat{\alpha}_1 - \hat{\alpha}_2$) in the horizontal plane.

Using the transmission equation of Harold Fris, we can obtain an expression for inclined range calculation r_{1incl} to the RES, which looks as follows:

$$r_{1incl} = \frac{ct_d \left(\frac{P_1}{P_2}\right)^{1/2}}{1 - \left(\frac{P_1}{P_2}\right)^{1/2}}, \quad (8)$$

where t_d is the delay time of the signal arrival to the second receiving element relative to the first one; P_1, P_2 are powers of the signal from RES received respectively by the antennas of RRM 1 and RRM 2.

It should be noticed that the inclined ranges to the first and the second receiving elements are related by the equation:

$$r_{2incl} = r_{1incl} + ct_d, \quad (9)$$

where r_{1incl} is the inclined range to the first receiving element from the location of the RES; r_{2incl} is the inclined range to the second receiving element from the location of the RES; c is the speed of light.

Respectively, mathematical equations for calculating elevation angles at the reception point A and B (Fig. 3) looks as follow:

$$\varepsilon_1 = \arcsin\left(\frac{H}{r_{1incl}}\right), \quad (10)$$

where H is the height of the radio receiver location at the instant of the signal received from the RES (Fig. 1):

$$\varepsilon_2 = \arcsin\left(\frac{H}{r_{2incl}}\right). \quad (11)$$

Formulas for calculating magnitudes of the projections of the inclined ranges from RES to the points A and B on the horizontal plane according to Fig. 3 can be presented as:

$$r_{1h} = \frac{H}{\operatorname{tg}(\varepsilon_1)} = \frac{H}{\operatorname{tg}\left(\arcsin\left(\frac{H}{r_{1incl}}\right)\right)} = \frac{H\sqrt{1-\left(\frac{H}{r_{1incl}}\right)^2}}{\left(\frac{H}{r_{1incl}}\right)} = \sqrt{r_{1incl}^2 - H^2} \quad (12)$$

$$r_{2h} = \frac{H}{\operatorname{tg}(\varepsilon_2)} = \frac{H}{\operatorname{tg}\left(\arcsin\left(\frac{H}{r_{2incl}}\right)\right)} = \frac{H\sqrt{1-\left(\frac{H}{r_{2incl}}\right)^2}}{\left(\frac{H}{r_{2incl}}\right)} = \sqrt{r_{2incl}^2 - H^2} \quad (13)$$

With an account of the equations (12)–(13), the angle between directions at the signal receiving points relative to the location point of the RES in the horizontal plane is calculated as (Fig. 1):

$$\Delta = (\alpha_1 - \alpha_2) = \arccos\left[\frac{r_{1h}^2 + r_{2h}^2 - (I^2 + (d - Vt_d)^2)}{2 \cdot r_{1h} \cdot r_{2h}}\right] \quad (14)$$

In the given case when the parameters $V_1, V_2, (d, I)$ (distance and the interval between the radio receivers carriers at the points A and B in Fig. 3) are *a priori* known, angle Δ is calculated according to (14); as f_{rec1} i f_{rec2} are measurable, then arrival direction of the signals and their carrier frequencies is unambiguously determined by the expressions (16)–(17) based on solving the system of equation presented below:

$$\begin{cases} f_{rec1} = f_{car} \left[1 + \frac{V_1}{c} \cos \alpha_1 \right] \\ f_{rec2} = f_{car} \left[1 + \frac{V_2}{c} \cos(\alpha_1 + \Delta) \right] \end{cases} \quad (15)$$

$$\alpha_2 = \alpha_1 + \Delta; V_1 = V_2 = V,$$

$$\Delta = \arccos \left[\frac{r_{1h}^2 + r_{2h}^2 - (d - Vt_d)^2}{2 \cdot r_{1h} \cdot r_{2h}} \right] = \arccos A_\Delta \quad ; \quad \begin{cases} f_{rec1} \\ f_{rec2} \end{cases} = \begin{cases} \left[1 + \frac{V}{c} \cos \alpha_1 \right] \\ \left[1 + \frac{V}{c} \cos(\alpha_1 + \Delta) \right] \end{cases}$$

$$f_{rec1} A_\Delta \cos(\alpha_1) - f_{rec1} \sqrt{1 - A_\Delta^2} \sin(\alpha_1) - f_{rec2} \cos \alpha_1 = \frac{c(f_{rec2} - f_{rec1})}{V}$$

Let us designate:

$$\begin{aligned} f_{rec1} A_\Delta &= f_{rec1} \left[\frac{r_{1h}^2 + r_{2h}^2 - (d - Vt_d)^2}{2 \cdot r_{1h} \cdot r_{2h}} \right] = A \\ f_{rec1} \sqrt{1 - A_\Delta^2} &= f_{rec1} \sqrt{1 - \left[\frac{r_{1h}^2 + r_{2h}^2 - (d - Vt_d)^2}{2 \cdot r_{1h} \cdot r_{2h}} \right]^2} = B \\ f_{rec2} &= C \\ \frac{c(f_{rec2} - f_{rec1})}{V} &= G \end{aligned}$$

$$A \cos \alpha_1 - B \sqrt{1 - \cos^2 \alpha_1} - C \cos \alpha_1 = G; \quad \cos \alpha_1 = t.$$

$$(A^2 + C^2 + B^2)t^2 + (2CG - 2AC - 2AG)t + (G^2 - B^2) = 0$$

$$t_{1,2} = \frac{-(2CG - 2AC - 2AG) \pm \sqrt{(2CG - 2AC - 2AG)^2 - 4(A^2 + C^2 + B^2)(G^2 - B^2)}}{2(A^2 + C^2 + B^2)}$$

Now we can introduce the restrictions: $\begin{cases} -1 \leq t \leq 1 \\ 0 \leq \alpha_1 \leq \pi \end{cases}$.

Thus, the equations for calculating the bearing angle at RES and its carrier frequency can be presented as:

$$\alpha_1 = \arccost \quad (16)$$

Under the condition that OX axis of the rectangular coordinates system XOY, depicted in Fig. 5, is oriented in parallel with the movement trajectory of the receiving elements of the radio monitoring system, with the ground site for collecting and processing of the radiolocation information (GSCPRLI) located at its center, coordinates of the RES location can be calculated as follows:

$$\begin{cases} x_{RES} = x_1 - \sqrt{r_{incl}^2 - H^2} \cdot \sqrt{1 - \left(\frac{c}{V_1}\right)^2 \left[\frac{f_{rec1}}{f_{car}} - 1\right]^2} \\ y_{RES} = y_1 + \sqrt{r_{incl}^2 - H^2} \cdot \frac{c}{V_1} \left[\frac{f_{rec1}}{f_{car}} - 1\right] \end{cases} \quad (18)$$

Implementation of the spatial location of the signal reception points (A and B) relative to RES (Fig. 4) can be secured due to respective radio control of the RRM carriers and is reduced to defining and transmitting control commands (CC) onboard the RES carrier with a fixed delay time relative to the CC of the leading object.

This task is characterized by the fact that the flight control is performed uninterruptedly along the whole flight trajectory of the grouping of the RRM carriers. To simplify the analysis, the above problem is considered in a single plane.

Locations of the leading and the led RRM carriers are determined in the inertial coordinates system with the axis H, P, D (\vec{V}). Leading carrier of RRM (LRRM) travels with the speed \vec{V}_1 at the height H_1 .

Similarly, the speed of the led RRM is $\vec{V}_2 = \vec{V}_1$, and the direction of its movement coincides with that of the leading RRM as well. From this follows that the angle of the trajectory inclination $\hat{\theta}$ equals the course angle of the leading RRM. This is true in the case when the attack angle equals zero and is illustrated by the kinematic ratios shown in Fig. 6.

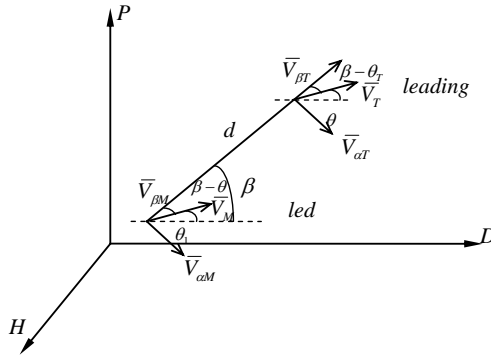


Fig. 6. Graphic interpretation of the kinematic ratios for the moving both leading and led RRM

The viewing angle in Fig. 5 is designated as β , the distance between the leading and the led RRM d ; the projections of the speed vector of the leading and the led RRM on the viewing line V_{BT} , V_{BM} , those on the normal to the viewing line V_{aT} , V_{aM} .

The role of the retaining system (RS) of the led RRM on the required trajectory is to form such CC (for the autopilot) that would keep the led RRM in the specified position of the grouping even when the leading one undertakes maneuvers.

Let us assume that the RS processes the incoming signal that equals (proportional) to the angle of the viewing line β or the viewing speed $\dot{\beta}$.

For such input signals, only one implementation of the control rule that can be used to retain the leading RRM in the position is possible, which is pursuit.

In this case, the led RRM is always located behind the leading one, that is $\theta = \beta$.

When any maneuver is absent, which means that the led RRM moves with the constant side speed, then with the constant longitudinal speed “ideal” distance between the two objects on the straight line is secured.

Following data in Fig. 5, kinematic ratios are as follows:

$$V_{\beta T} - V_{\beta M} = V_T \cos(\beta - \theta_T) - V_M \cos(\beta - \theta) = \dot{d} \quad (19)$$

$$d = d_0 + \dot{d}\Delta t,$$

while the angle deviations are:

$$\dot{\beta} = -\frac{V_{aT} - V_{aM}}{d} = -\frac{V_T \sin(\beta - \theta_T) - V_M \sin(\beta - \theta)}{d} \quad (20)$$

$$\beta = \beta_0 + \dot{\beta}\Delta t$$

The method of “clear” pursuit is characterized by the fact that neither leading nor led RRM makes any maneuvers. Then, it is obvious that $V_T = \text{const}$, and $\theta_T = 0$, $\theta = \beta$.

In this case:

$$\frac{d(d)}{dt} = V_T \cos\beta - V_M = \dot{d};$$

$$\dot{\beta} = \frac{d\beta}{dt} = -\frac{V_T \sin\beta}{d} \quad (21)$$

For the above formulas, $\dot{\beta}$ equals zero only if $\beta = 0$ or π , so the pursuit is performed exactly in “the tail.”

Solution for β and the trajectory inclination angle θ , as a function of the distance d , looks as follows:

$$\frac{d(d)}{d\beta} = \left(-ctg\beta + \frac{V_M}{V_T} \text{cosec}\beta\right) d \rightarrow \frac{d(d)}{dt} = (-ctg\beta + \gamma \text{cosec}\beta) d\dot{\beta}, \quad (22)$$

where $\gamma = \frac{V_M}{V_T}$ is the ratio of the speeds of the leading and the led CRRM.

Reverse transformation of (22) can be presented as:

$$\ln d = -\ln|\sin\beta| + \gamma \ln \left| \text{tg} \frac{\beta}{2} \right| + \text{const} \quad (23)$$

if assumed that $0 \leq \beta < \pi$, then

$$\ln \frac{d \sin \beta}{\operatorname{tg}(\frac{\beta}{2})^\gamma} = \text{const}, \quad (24)$$

or

$$\frac{d \sin \beta}{(\operatorname{tg} \beta / 2)^\gamma} = \frac{d_0 \sin \beta}{(\operatorname{tg} \beta_0 / 2)^\gamma} = k = \lambda, \quad (25)$$

where d_0 and β_0 are required values of the distance and the viewing angle of the led CRRM relative to the leading one.

Because both the leading and the led CRRM have to be on the same line, then β approaches zero, and $k = \lambda$ should be constant.

The exact approach “at the tail” of the leading CRRM takes place under the condition: $\beta = \theta = 0$:

$$\dot{\beta} = -\frac{v_T}{\lambda} \frac{(\sin \beta)^2}{(\operatorname{tg} \beta / 2)^\gamma}.$$

On the segment of the trajectory where $\beta \ll 1$, $\sin \beta \approx \beta$, $\operatorname{tg} \frac{\beta}{2} \approx \frac{\beta}{2}$, an expression for the angular velocity looks as follows:

$$\dot{\beta} \approx \frac{2^\gamma (v_T)}{\lambda} - \gamma.$$

Implementation of the CRRM movement in parallel courses with the set interval (I) and the distance (d) between them, on the selected monitoring time intervals, permits to substantially increase their noise immunity due to the multi-positional reception of the location information from the RES.

In this type of homing, for each led RRM, fixed magnitudes of the angle β and the interval I are set; in other words, the constant advance angle is created (Fig. 7).

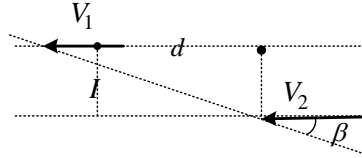


Fig. 7. Projections of the trajectories of the two CRRM with the given interval (I) and the distance (d) between them on the horizontal plane.

Fig. 8 demonstrates the probable trajectories of CRRM by the values of γ .

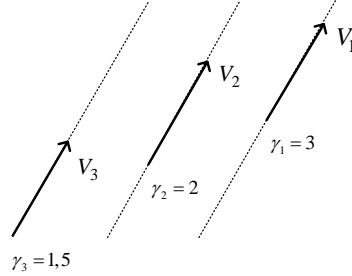


Fig. 8. Probable trajectories of the CRRM by the values of γ .

When led CRRMs to move at a constant speed, they pursue without maneuvering the leading one on a parallel course. This secures the constant nature of the trajectory, in other words, fixed angle β_n .

Thus, pursuit with a fixed angle also makes sense, as in the case of the “clear” pursuit, but for the starting conditions when $\beta \leq \frac{\pi}{2}$.

For the implementation of the pursuit with a constant angle, information about the speed ratio of the leading CRRM to the led one is required, as well as attack angles.

If the attack angle is constant, viewing lines does not change as well, that is $\dot{\beta} = 0$.

It is possible in the case when the speed component $V_{\alpha T}$ of the led CRRM that is located behind the normal to the viewing, the line is balanced by the normal speed component $V_{\beta T}$ of the led one. In this case angular accelerations $\dot{V}_{\alpha T}$ and $\dot{V}_{\beta T}$ do not occur and the led CRRM never overtakes the leading one.

To realize such a control method, which is similar to the parallel approach, CCs are defined as follows:

$$\lambda = \frac{\dot{\theta}}{\dot{\beta}} \quad (26)$$

Nevertheless, for the parallel approach method, CCs are constantly applied, while for the method of approach with a constant angle they are used only under the condition of acceleration, which is when $\dot{\theta} = 0, \dot{\beta} = 0$.

CCs level is defined by the ratio

$$\theta = \lambda\beta + \theta_0 \quad (27)$$

where θ_0 is an initial angle of the divergence.

In this case, the CCs level can be calculated through γ :

$$\sin(\beta_0 - \theta_0) = \frac{V_T}{V_M} \sin(\beta_0 - \theta_T) \Rightarrow \sin(\beta_0 - \theta_0) = \gamma \sin(\beta_0 - \theta_T) \Rightarrow \lambda = f(\gamma) \quad (28)$$

Movement trajectory of CRRM for $\gamma = \frac{V_M}{V_T} = 2$ and corresponding control commands $2\lambda, 4\lambda, 6\lambda$ are shown in Fig. 9.

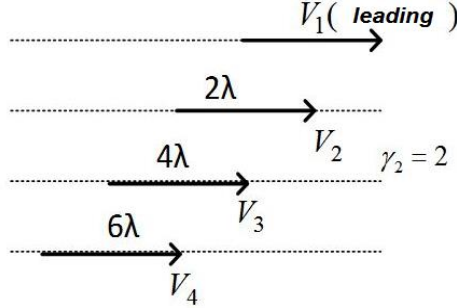


Fig. 9. Trajectories of CRRM for $\gamma = 2$ and the respective CC (2λ , 4λ , 6λ)

Implementation of the presented trajectories is possible only in the ideal control system for any initial conditions.

To calculate reference trajectories, it is necessary to assume that the movement of the led CRRM is performed on the time interval $t_n = 0 + \Delta t$ with constant speed V_M and such angles of the trajectory inclination θ that they are directed along the trajectory of the leading CRRM.

If $V_{\beta M}$ represents the speed component of the led CRRM that is directed along the trajectory of the leading one, and the side component $V_{\beta T} \approx 0$, then the expression for the speed of the carrier descent can be presented as follows:

$$\dot{d} = V_{\beta T} - V_{\beta M} = \text{const.} \quad (29)$$

From above, the formula for the distance between the led carriers is as shown below:

$$d = d_0 - |V_{\beta T} - V_{\beta M}| t \quad (30)$$

where d_0 is that value of the initial distance for which approach speed is constant or equals zero.

Delay time of the CC issuing is defined as follows:

$$t_i = \frac{d_0}{|V_{\beta T} - V_{\beta M}|} \quad (31)$$

But the presence of the angular velocities of CRRM and delays in CC issuing leads to deviation of the real trajectory from the reference one. This deviation at a certain time instant t manifests itself by the perpendicular shift y_t .

Similarly, the longitudinal location of the led CRRM is determined by the value of the deviation y_m .

Deviation of the trajectory of CRRM in time is also characterized by the velocities \dot{y}_m , which are defined by the fluctuations of the angle θ .

If the trajectory of the CRRM is kept in the space angle $\theta \ll 1^\circ$, then the shift speed can be determined by the dependence:

$$\begin{aligned}\dot{y}_m &= V_M \theta \cos \theta = V_{\beta M} \theta \\ y_t &= y_{0t} + \dot{y}_m \Delta t = y_{0t} + \dot{y}_m t_i\end{aligned}\quad (32)$$

In practice, the realization of the pursuit with an angular shift is possible based on the autopilot (AP) with dynamic delay.

If the operation of the AP is considered as that of a linear device, then the CC level with the account of the errors can be expressed as follows:

$$\lambda = \frac{\theta}{y_m \beta} \quad (33)$$

and the distance error:

$$\begin{aligned}\beta &= \frac{y_t - y_m}{d} \quad d \gg (y_t - y_m) \\ d &= \frac{y_t - y_m}{\beta}\end{aligned}\quad (34)$$

The retention error in the required angle range (DC RRM):

$$\begin{aligned}\theta &= \frac{\dot{y}_m}{V_{\beta M}}; \\ \theta &\ll 1^\circ\end{aligned}\quad (35)$$

Retention of the led RRM at a respective distance is possible by deploying a radio beam (RB) (on the viewing line).

In this case, the led CRRM move in the range of line-of-sight of the leading CRRM.

To perform the movement along the viewing line, the speed $V_{\alpha M}$ of the leading CRRM has to equal the linear speed $d_T \dot{\beta}$, where d_T is the distance from the leading CRRM to the led one. In this case:

$$V_{\alpha M} = d_T \dot{\beta} \Rightarrow \dot{\beta} = \frac{V_{\alpha T}}{d_T} \quad (36)$$

In the case when the led CRRM moves along the set trajectory (is in the range of the radio beam) $d_T \approx const$ and $V_{\alpha M} = 0$, then the situation is similar to the case of the “clear” pursuit, but with the shift.

When the led CRRM deviates from the required trajectory $d_T \neq const$; $V_{\alpha M} \neq V_{\alpha T}$, it is namely this that presents itself as a discrepancy parameter for the flight control system (FCS) of the led CRRM.

The main advantage of the pursuit method with the shift in its simplicity. The principal drawback of this method is the emergence of the errors when delay distance for the led CRRM increases.

Dynamic error (failure) of retaining led CRRMs on the required trajectory for both the case of the “clear” pursuit and the pursuit with the shift is as follows:

$$M = y_i(t_i) - y_m(t_i) \quad (37)$$

where t_i is the factual delay time of the CC arriving on board of the led CRRM.

Delay time of CC must not surpass the time of the complex time constant of the control loop of the aerodynamic object T_e , so $t_i < T_e$, and in an ideal case $t_i \ll T_e$; this is because, in the general incident, the processing time of CC and working out control decisions will be defined as $t_i + T_e$, hence for t_i to be by order less than T_e , will secure the required quality of functioning of FCS of the led CRRM.

4 Conclusions

Mobile means of radio monitoring functionally complement the stationary ones and provide flexible support for effective radio monitoring when radio emissions parameters are measured from beyond their accessibility zone. Utilization of the mobile systems of the radio monitoring based on the mobile radio-controlled modules for performing practical tasks permits to more successfully carry out radio spectrum control and reveal unlicensed radio transmissions.

Concerning this, the problems of studying achievable potential limits of the passive radio monitoring methods with synthesized apertures remain topical and important for practical implementations. Radio monitoring tasks can be performed with the help of deploying passive radiolocation systems; those systems can include not one but quite a few spatially diversified radio-controlled receiving modules.

The necessary condition of solving the task of determining coordinates of RES by the designed system is the deployment of at least three mobile radio receiving modules during the monitoring time interval. In this system, the information that is received by the separate radio locating measurers is processed together. The algorithms analyzed in this paper permit to reveal the coordinates of the radio emission sources in the passive mode and for non-directional reception. It should be stressed that the implementation of the presented algorithms is economically viable in comparison to the space systems of the radio monitoring, which perform the same technical tasks.

The efficiency of the proposed dynamic models depends not only on the parameters of the radio reception modules but also on the characteristics of the signals from the sources of the radio emissions. A substantial role in all this is played by the ratio between the parameters of the antenna movements of the RRM and the measured signal coherency interval. If the phase structure of the signal does not degrade on the entire space-time monitoring interval, then, due to taking into account *a priori* known information on the movement parameters of the radio locating measurers, it is possible to substantially increase the efficiency of the system in resolving the analyzed problem.

References

1. Druzhinin, V.: Forming and Processing Radar Information in Radiovision Systems (2013)
2. Druzhinin, V., et. al.: Methods and Algorithms of Information Processing and Protection in Radar Systems with Adjustable Space Configuration (2014)
3. Gorban, I. Processing of Hydroacoustical Signals Under Complex Dynamic Conditions (2008)
4. Karavaev, V. V., Sazonov, V. V.: Statistics Theory for Passive Location (1987)
5. Hayes, M. P., Gough, P. T.: Synthetic aperture sonar: a review of current status. *IEEE J. Ocean. Eng.* **34**(3): 207–224 (2009)
6. Autrey, S. W.: Passive synthetic arrays. *IEEE J. Ocean. Eng.* **84**(2): 592–598 (1988)
7. Stergiopoulos, S.: Optimum bearing resolution for a moving towed array and extension of its physical aperture. *J. Acoust. Soc. Am.* **87**(5): 2128–2140 (1990)
8. Edelson, G. S., Tufts, D. W.: On the ability to estimate narrow-band signal parameters using towed arrays. *IEEE J. Ocean. Eng.* **17**(1): 48–61 (1992)
9. Ivanenkov, A. S., et al.: Cramer–Rao lower bound for localization of a source with partial temporal coherence using passive synthetic aperture. 12th European Conference on Underwater Acoustics: 564–571 (2012)